

## Highly elastic aerogel derived from spent coffee grounds as oil removal adsorbent

Yongli Chen\*, Weijie Cai\*, Meng Zhang\*, Meiyong Xie\*\*\*, Fengzhi Tan\*<sup>†</sup>, and Fan Yang\*\*\*\*<sup>†</sup>

\*School of Light Industry and Chemical Engineering, Dalian Polytechnic University, Dalian 116034, China

\*\*CAS Key Laboratory of Design and Assembly of Functional Nanostructures,  
and Fujian Provincial Key Laboratory of Nanomaterials, Fujian Institute of Research on the Structure of Matter,  
Chinese Academy of Sciences, Fuzhou, Fujian 350002, China

\*\*\*Xiamen Institute of Rare Earth Materials, Haixi Institute, Chinese Academy of Sciences, Xiamen, Fujian 361021, China

(Received 8 September 2021 • Revised 20 December 2021 • Accepted 22 December 2021)

**Abstract**—In the face of increasing environmental pollution, aerogels have emerged as valuable materials for potential oil/water separation. However, many of the currently developed aerogels have unsatisfactory compressibility, high cost and a single hydrophobic modification method, which limits larger-scale application. In this work, a type of aerogel with compressible, inexpensive, and fully biodegradable features was designed via a novel zirconium chloride modification strategy. Typically, a series of aerogels (HCSW-1, HCSW-2, and HCSW-3) were readily prepared from a mixture of spent coffee grounds, waste paper and sodium alginate. The prepared aerogels exhibited good elasticity, low density ( $0.024 \text{ g cm}^{-3}$ ), high porosity (98.3%), efficient oil/water separation and good oil uptake (23–44 times of its weight). In addition, the as-prepared aerogels can be easily recycled several times, thus meeting the demand of actual oil/water separation. Such prominent results provide a new perspective for the development of efficient hydrophobic aerogels in the treatment of offshore oil spills and industrial wastewater.

Keywords: Bio-based Aerogel, Spent Coffee Grounds, Hydrophobic Modification, Oil/Water Separation

### INTRODUCTION

In recent decades, human activities have caused serious environmental pollution, especially water pollution. According to recent research data, the level of oil pollutants in the discharged effluent has continuously increased over the years [1–4]. Oil leakage not only can pollute the natural environment of coastal cities but lead to a waste of resources as well as endangering human health. To resolve this problem, various methods have been developed, including membrane filtration [5], ion exchange [6], and reverse osmosis [7]. Although these methods can tackle the problem to some extent, their application is still limited because of the potential secondary pollution and high cost. Among the developed treatment techniques, the adsorption method is an attractive choice due to its good oil removal ability, environmentally friendly property, low-cost, high efficiency, and easy operation [8,9]. Therefore, it is imperative to design an economical and biodegradable adsorption material. Adsorption refers to the accumulation or condensation of one or more components of a fluid (gas or liquid) mixture on the surface with porous solids (adsorbents) for separation [10]. At present, activated carbon/alumina, aerogel and composite adsorption materials are commonly used as adsorbents for sewage treatment. Among them, aerogel-type adsorbents with ultra-low density, ultra-high porosity and excellent adsorption capacity have attracted extensive attention. Presently, various aerogels have been developed as oil sorbents, including organic aerogel [11], inorganic aerogel [12], composite aerogel [13]. How-

ever, there are some defects in organic aerogels, such as brittleness and poor biodegradability. Additionally, the preparation process of inorganic aerogel is complex and its oil adsorption ability is unsatisfactory. Although composite aerogels exhibit certain oil-water separation performance, their high cost and complex fabrication process still limit their further application. Meanwhile, it has been evidenced that composite aerogel often requires the doping of costly graphene materials. Hence, it is urgent to develop a low-cost, environmentally friendly, and simple way to synthesize the biomass-derived aerogel.

Spent coffee grounds (SCG), as waste biomass resources, are estimated to be approximately 8 million tons every year [14,15]. However, most of the SCG are directly discarded as valueless wastes; thus it is meaningful to convert these wastes into value-added materials through appropriate modification methods. At present, SCG is used as the substrate for adsorption because of its loose and porous structure and various functional groups that can be adsorbed. In contrast, the aerogel directly prepared from SCG often suffers from sample shrinkage and a difficulty for shape control. This could be interpreted by the fact that the larger coffee ground particles tend to sink before the solution freezes. Therefore, wastepaper (WP) was selected to solve this problem. WP is rich in cellulose fibers, which can act as good structural support for aerogels [16]. However, these materials are hydrophilic, thereby requiring hydrophobic modification to improve the oil-water separation capacity. Generally, hydrophobic methods include atomic layer deposition [17], chemical vapor deposition [18] as well as high-temperature carbonization [19]. Among them, chemical vapor deposition is the most used hydrophobic modification method. But this technique is flammable, explosive, and harmful. To avoid potential hazards, a new hydrophobic modification method is explored by spraying with some

<sup>†</sup>To whom correspondence should be addressed.

E-mail: tanfz@dlpu.edu.cn, fanyang2013@fjirsm.ac.cn

Copyright by The Korean Institute of Chemical Engineers.

non-toxic or less toxic reagents. However, aerogels still possess have poor mechanical properties. Repeated tests revealed that the addition of sodium alginate (SA) significantly improved its mechanical properties, due to the crosslinking with cellulose. Moreover, it can also be further cross-linked with metal ions to form stronger ionic bonds, thereby obtaining better mechanical properties [20]. Simultaneously, the SA is non-toxic, biodegradable, and cost-effective [21]. Therefore, the combination of SCG, WP and SA to prepare new hydrophobic aerogels will be promising in the field of oil/water separation.

In this work, a light weight, compressible, and bio-based aerogel was prepared through a simple suspension dispersion. The aerogel was derived from renewable biomass materials and modified by a novel hydrophobic method. The characterization results revealed that the aerogel possessed a multilayer interconnected porous structure and good thermal stability. The optimized aerogel exhibited good elasticity, high hydrophobicity, and excellent oil/water selectivity. Moreover, aerogels can also be easily recycled.

## MATERIALS AND METHODS

### 1. Materials

SCG was obtained from Dalian Man Coffee Catering Management Co., LTD. The waste paper was purchased from a local market in Dalian, China. SA was purchased from Tianjin Guangfu Fine Chemical Research Institute. Zirconyl chloride octahydrate ( $ZrOCl_2 \cdot 8H_2O$ , 98%,  $M_w=322.25$ ) was purchased from Alighting Reagent (Shanghai) Co., LTD. Sodium hydroxide (NaOH) was obtained from Kermel Chemical Reagent Co., Ltd (Tianjin, China). N-hexane, carbon tetrachloride, kerosene was purchased from Tianjin Kemiou Chemical Reagent Co., LTD. Soya bean oil, crude oil, corn germ oil, etc. were purchased from a local market in Dalian, China. All chemicals were of analytical grade and directly used without further purification.

### 2. Pre-treatment of Raw Materials

A certain amount of SCG was first added into 1 M NaOH aqueous solution, stirred at 80 °C for 3 h, filtered and then the precipi-

**Table 1. Physical features of CSW materials (CSW-1, CSW-2, CSW-3)**

Samples	SCG (wt%)	WP (wt%)	SA (wt%)	Density ( $g\ cm^{-3}$ )	Porosity (%)
CSW-1	1	0.7	0.3	0.024	98.3
CSW-2	1	0.6	0.4	0.036	97.4
CSW-3	1	0.5	0.5	0.039	97.2

tates were washed with deionized water until filtrate was neutral. Subsequently, the obtained precipitates were dried and ground. The WP was crushed with a grinder and dried for further use.

### 3. Preparation of SCG/SA/WP Aerogel (CSW)

0.3 g of SA was added in 98 mL deionized water and then stirred until a homogeneous aqueous solution was obtained. A mixture containing 1 g of pretreated SCG with alkali and 0.7 g of WP was introduced in SA solution and stirred for 1 h. Then, the mixture was suspended and dispersed at high speed for 0.5 h, followed by ultrasonic treatment for 15 min. Subsequently, the mixture was poured into a mold for rapid freezing in a cryogenic refrigerator at  $-40\ ^\circ C$  and then dried in a freeze-dryer for 36 h to obtain aerogel CSW-1. Similarly, the aerogel CSW-2 and CSW-3 were prepared by setting the mass ratio of SCG, SA and WP as 1:0.4:0.6 or 1:0.5:0.5. Their densities and porosities are listed in Table 1. The detailed preparation process is shown in Fig. 1.

### 4. Preparation of Hydrophobic SCG/SA/WP Aerogel (HCSW)

The prepared composite aerogel was hydrophobically modified using 3 wt%  $ZrOCl_2 \cdot 8H_2O$  solution. As a facile preparation method, the aerogel was sprayed with  $ZrOCl_2 \cdot 8H_2O$  solution, and then dried in an oven. The hydrophobic aerogel was obtained by repeated operation for three times. The resulting sample was denoted as HCSW-1, HCSW-2 and HCSW-3, respectively. The preparation process is shown in Fig. 1.

### 5. Characterization

The surface morphology of the samples was analyzed by scanning electron microscope (SEM, JSM-6460LV) with X-ray energy spectrum (EDS). The functional groups were identified by Fourier

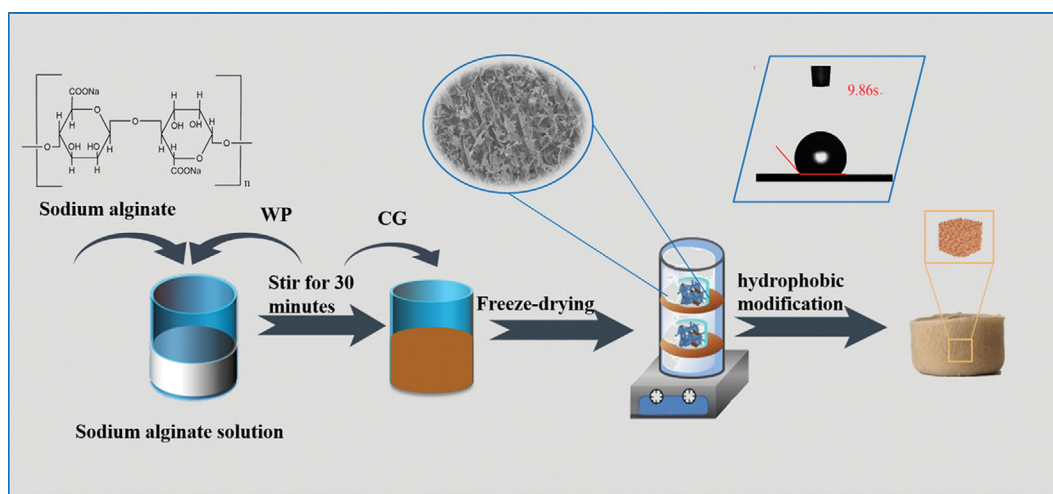


**Fig. 1. Schematic illustration of the preparation of aerogel.**

transform infrared spectrometer (FT-IR). The hydrophobic property of the sample was determined and evaluated by the contact angle tester (Biolin Science Co., Ltd., Finland).

The quality and dimensions of aerogels were measured using scales and vernier calipers and apparent density was calculated by Eq. (1):

$$\rho = \frac{m}{\pi r^2 D}, \quad (1)$$

where  $\rho$  is the aerogel density ( $\text{g}\cdot\text{cm}^{-3}$ ),  $m$  is to the aerogel mass (g),  $r$  is to the aerogel radius and  $D$  is the aerogel thickness (cm).

The porosity ( $P$ ) of aerogels was calculated by the following equation:

$$P = \left(1 - \frac{\rho}{\rho_0}\right) \times 100\%, \quad (2)$$

where  $P$  is the porosity of aerogel and  $\rho_0$  is the solid density of aerogel. Based on the reported data in the literature, the density of

cellulose ( $1.500 \text{ g cm}^{-3}$ ) and SA ( $1.000 \text{ g cm}^{-3}$ ) was selected as the solid density [22].

## 6. Evaluation of Adsorption Capacity and Recyclability

To evaluate the adsorption properties of aerogels, various oils and organic solvents were selected for adsorption. First, a certain amount of oil or organic solvent was poured into the beaker, then the aerogels (initial mass was recorded as  $m_0$ ) were immersed into the solvent system. After adsorption for a while, the aerogels were taken out and placed for 1min until no oil-dropping. Each sample was weighed and repeated for three times. The calculation formula of the oil adsorption ratio was as follows:

$$Q = (m - m_0) / m_0 \quad (3)$$

where  $Q$  ( $\text{g g}^{-1}$ ) is the adsorption ratio of the aerogel to oil or organic solvent;  $m$  (g) is the weight of the aerogel after the adsorption of the oil or organic solvent;  $m_0$  (g) is the mass of the aerogel.

The recyclability of the aerogel can be judged by the adsorption capacity after ten consecutive adsorption-desorption cycles. Desorp-

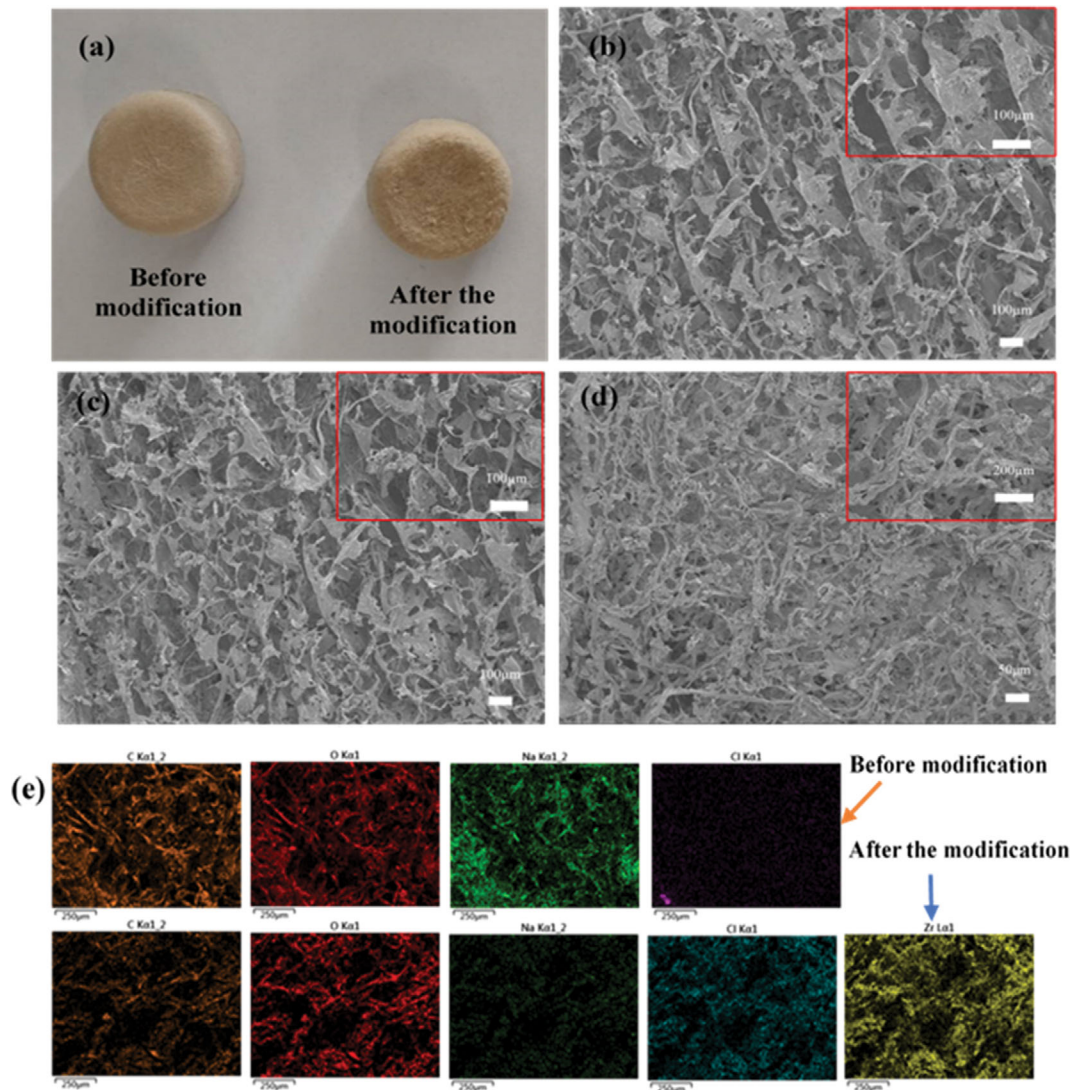


Fig. 2. Microstructure of aerogels. (a) Photograph before and after aerogel modification. SEM images of: (b), (c) CSW-1, (d) HCSW-1. (e) EDS images of CSW-1 and HCSW-1.

tion tests can be conducted by simply squeezing and soaking in ethanol. In this paper, tetrachloromethane was used in a reproducible experiment to determine its adsorption performance after ten cycles.

## RESULTS AND DISCUSSION

### 1. Characterization

The density and porosity of the samples are listed in Table 1. It can be seen that the prepared sample has a relatively low density of  $0.024 \text{ g cm}^{-3}$  and a high porosity of 98.3%. The surface area of the CSW-1 measured by BET was  $206.4 \text{ m}^2 \text{ g}^{-1}$  (Table S1). Differences in the specific surface area indicated that different additives could modulate the microstructure of aerogels, providing a convenient way to control the material structure.

Fig. 2(a) shows optical photos of aerogel before and after hydrophobic modification. After modification, it exhibited good hydrophobic properties, although no obvious change occurred in its appearance (Fig. S1). SEM images were collected to further prove its morphologic structure. The three-dimensional pore structure could be clearly observed in Fig. 2(b), (c). This wide-open porous structure provides adequate space for oil storage, while the layered structure supplies the vertical entry points for oil entry [23]. Indeed, SCG and WP are interconnected and intertwined to form a three-dimensional porous structure. The layer thickness increases with increasing SA, which might be due to the formation of complex dense structure. After modification, it can be found that the lamellae are interconnected, because the cross-linking effect of  $\text{Zr}^{4+}$  on SA made the film layer more thicker (Fig. 2(d)) [20].

FTIR analysis was used to identify the contained groups of the aerogel. The symmetric and asymmetric telescopic vibration peaks corresponding to the aliphatic hydrocarbons C-H at  $2,920 \text{ cm}^{-1}$  were weak, and the telescopic vibration peak of the fatty acids C=O in SCG disappeared at  $1,744 \text{ cm}^{-1}$ , indicating the disappearance of the fatty acids in coffee grounds after the alkali treatment [24] (Fig. S2). As shown in Fig. 3, the aerogel exhibits an obvious adsorp-

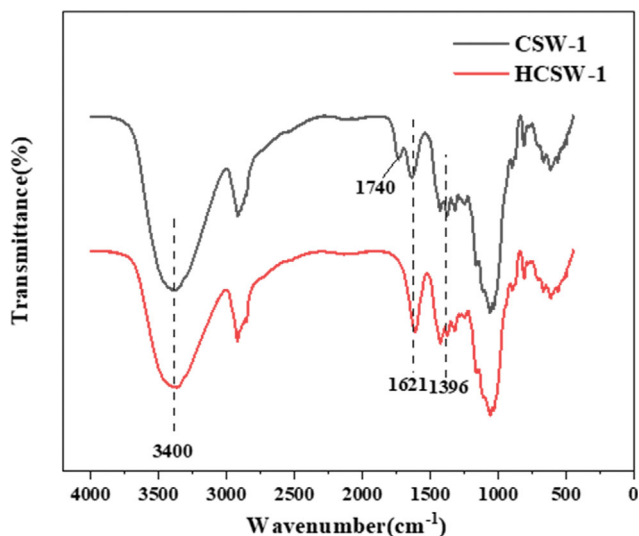


Fig. 3. FTIR spectra of CSW-1 and HCSW-1.

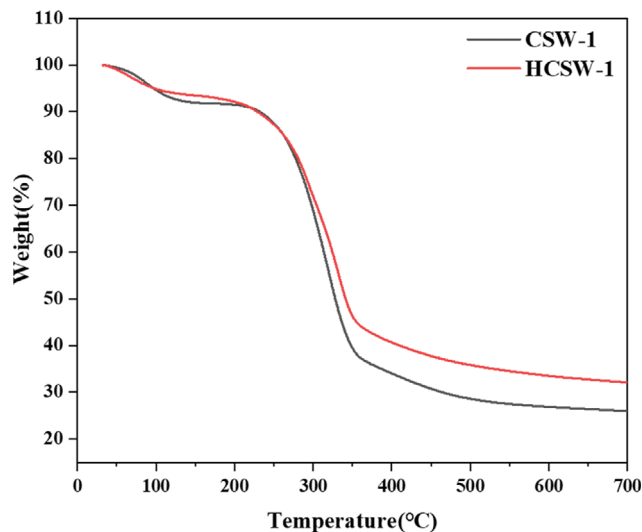


Fig. 4. TGA curves of CSW-1 and HCSW-1.

tion peak at  $3,400 \text{ cm}^{-1}$ , which corresponds to the O-H (including hydrogen bonding) telescopic vibration peak. The characteristic peaks of SA that appeared at  $1,621 \text{ cm}^{-1}$  and  $1,396 \text{ cm}^{-1}$  are assigned to asymmetric and symmetric vibrational bands of the carboxyl group (-COOH), respectively [25]. The appearance of a new peak at  $1,740 \text{ cm}^{-1}$  and a significant decline in peak intensity at  $1,621 \text{ cm}^{-1}$  suggests that it may be indexed with the chemical cross-linking of  $\text{-COO}^-$  and  $\text{Zr}^{4+}$  [26]. The cross-linking of  $\text{Zr}^{4+}$  ions and SA increased the surface roughness of the material and thus improved its hydrophobicity, which was consistent with the frontal SEM findings.

The thermal stability of aerogels is of great importance considering their thermal insulation applications. As shown in Fig. 4, a small weight loss below  $100 \text{ }^\circ\text{C}$  can be clearly observed due to the evaporation of moisture. In addition, the mass loss of aerogel at ca.  $200\text{--}450 \text{ }^\circ\text{C}$  corresponds to the structural decomposition of SCG and paper, such as hemicellulose, and lignin [27]. When further increasing temperature to  $700 \text{ }^\circ\text{C}$ , the mass loss of the CSW-1 is about 75%, while the loss is about 68% for HCSW-1, which indicates higher thermal stability of the modified aerogel.

### 2. Compressive Property

Generally, the good compression properties of aerogels are critical for practical applications. As shown in Fig. 5(a), the aerogel can withstand a weight as high as 200 g (720 times its weight), and still recover after unloading. Moreover, even if the sample is compressed and deformed by 50%, the shape of the sample is still maintained after the removal of the applied force (Fig. 5(b)). This high elasticity is mainly caused by the good entanglement of cellulose with SA, in accordance with the previous SEM results.

### 3. Determination of Wettability

Oil/water selectivity is a key property for oil sorbents [28]. As shown in Fig. 6(a), water (methylene blue stain) forms spherical droplets on the sample surface, while the soybean oil (Sudan III stain) rapidly permeates into the sample. In Fig. 6(b), the Soybean oil stained with Sudan III is mixed with water, and after the addition of the HCSW-1 sample, the oil in the water solution is com-

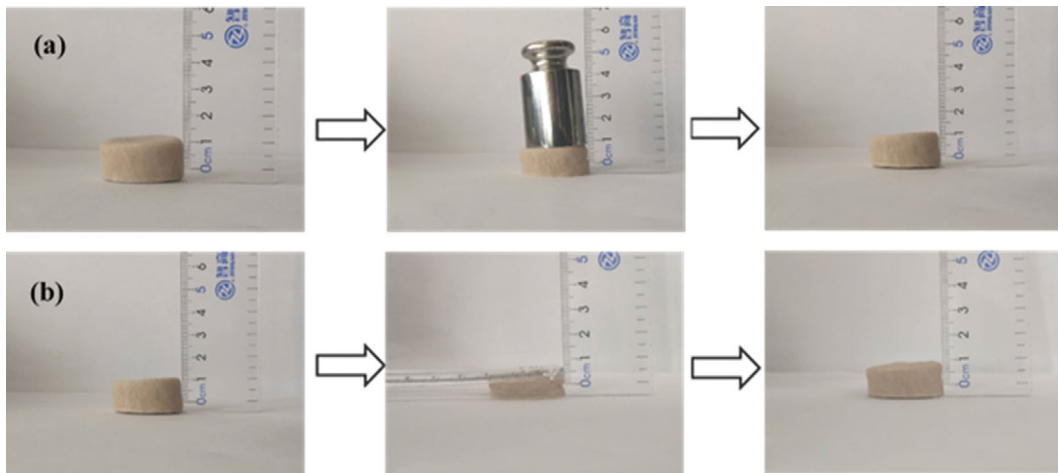


Fig. 5. Digital photographs illustrating the compressive properties of the HCSW-1 aerogel.

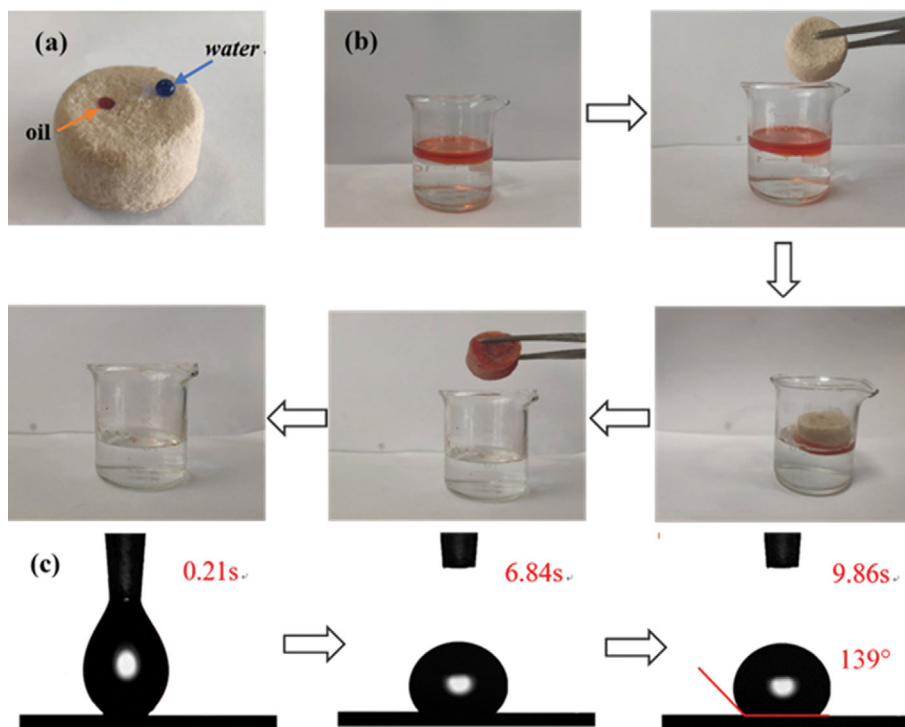


Fig. 6. (a) Hydrophobic photo of HCSW-1. (b) Selective removal of soybean oil (dyed red by Sudan III) from the water using HCSW-1. (c) The water contact angles of HCSW-1 at different times.

pletely adsorbed and removed within 1 min. The result shows that the modified sample presents good hydrophobic and lipophilic features. To accurately depict its hydrophobic properties, the water contact angle was measured. It is well accepted that the water contact angle is regarded as one of the important criteria for evaluating the performance of oil-adsorbent materials. When the contact angle is above  $90^\circ$ , the sample is regarded with hydrophobicity [29]. After the measurement of the contact angle, it was observed that the contact angle size was  $139^\circ$ , which exhibited its superhydrophobic feature (Fig. 6(c), film S1). In addition, no obvious change of the contact angle occurred with the extension of time, suggesting good hydrophobicity.

#### 4. Tests of Adsorption Capacity

The efficient elimination of oil and organic pollutants in water has received more and more attention [30]. The adsorption degree of various oil and organic solvents is correlated with the density of the adsorbed solvent as well as its pore structure. As previously depicted in the SEM findings, HCSW-1 material had a hierarchical porous structure, which could provide adequate capillary channels for oil adsorption and enough space for oil storage.

To start with, the adsorption capacity of different samples for soybean oil was tested. As shown in Fig. 7, the HCSW-1 sample presents a higher adsorption capacity compared with the others. Its adsorption multiplicity can reach  $26 \text{ g g}^{-1}$ . This result is closely

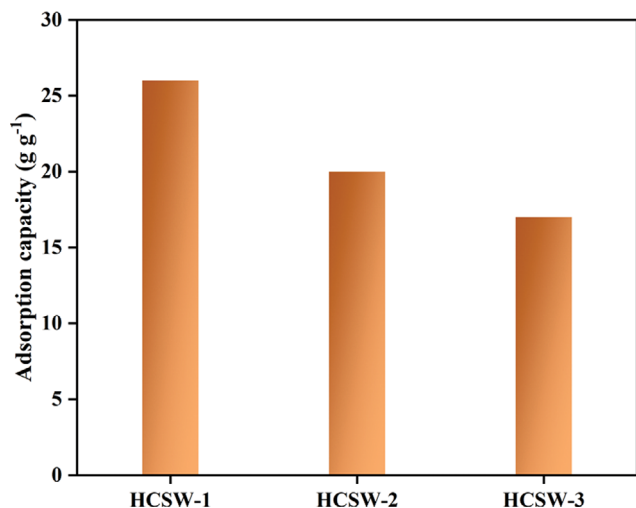


Fig. 7. The adsorption capacity of HCSW-1, HCSW-2 and HCSW-3.

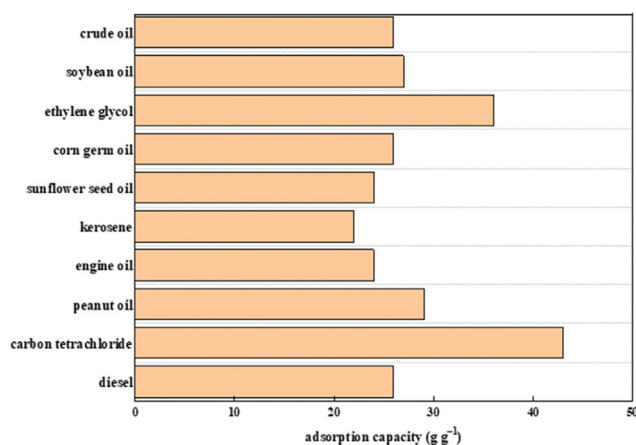


Fig. 8. The HCSW-1 adsorption capacity for various oils and organic solvents.

in line with the density and porosity of the sample. The adsorption multiplicity of sample CSW-1 is  $29 \text{ g g}^{-1}$ , which can be seen that the multiplicity decreases slightly after hydrophobic modification, but it still has high adsorption performance. Therefore, HCSW-1 was used as the predominant sample for the next test. Fig. 8 shows the adsorption capacity of the HCSW-1 sample for some common oils/organic solvents. It can be observed that the maximum adsorption capacity for carbon tetrachloride was  $44 \text{ g g}^{-1}$ , and the minimum adsorption capacity for kerosene was  $23 \text{ g g}^{-1}$ . The reason for this result is that the density and viscosity of  $\text{CCl}_4$  are relatively high and it was easy to enrich within the aerogel and the storage volume might be larger, while organic solvents or oils with less density and viscosity, such as kerosene, are not easy to enrich within the aerogel, thereby the adsorption capacity is lower. To conclude, these results revealed that the prepared HCSW-1 aerogel would be a promising adsorbent for oil-water separation.

Fig. 9 shows the adsorption capacity of HCSW-1 for sunflower seed oil and ethylene glycol with time on stream. It can be found that the adsorption rate of ethylene glycol is faster than that of sun-

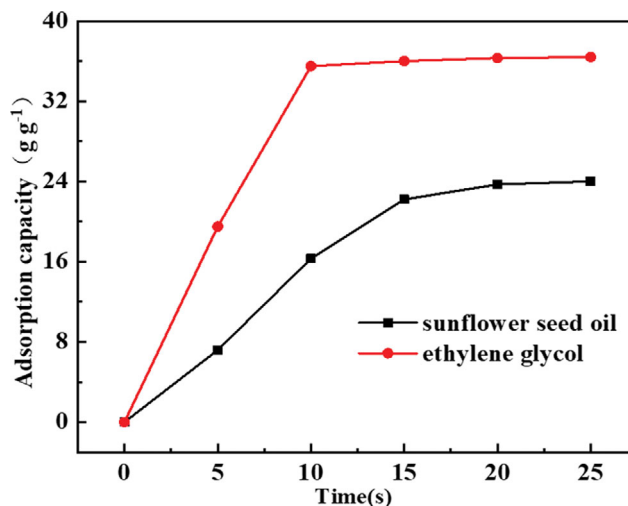


Fig. 9. The adsorption capacity of HCSW-1 for sunflower seed oil and ethylene glycol over time.

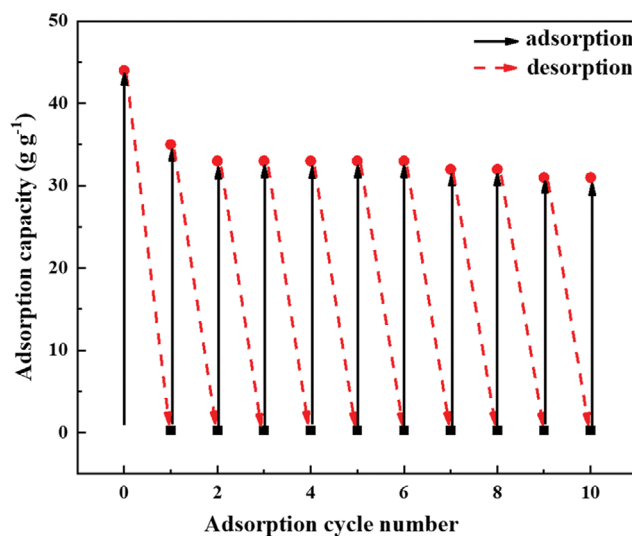


Fig. 10. Recyclability tests of HCSW-1 aerogel for carbon tetrachloride.

flower oil, because of the lower viscosity of ethylene glycol. On the contrary, the adsorption rate becomes slower upon further increasing the adsorption time, which might be explained by the fact that the adsorption sites inside the aerogel are gradually saturated with oil [31].

### 5. Recyclability Tests

The recyclability of the sorbent is a key factor for its potential pilot application [32]. In this work, carbon tetrachloride was selected as the model contaminant to investigate the cycling capacity of the HCSW-1 sample. Indeed, carbon tetrachloride was completely adsorbed by HCSW-1, and then compressed and dried to remove the adsorbed solvent for the next cycle. As shown in Fig. 10, after ten consecutive operations, the sample still maintained 71% of the original adsorption capacity, indicating its good recyclability.

To elucidate the influence of aerogel on the separation of oil-water emulsion, an experiment was conducted on toluene-water

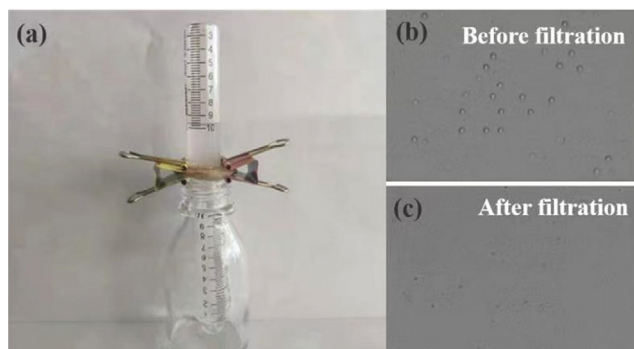


**Fig. 11.** Separation of water-in-oil emulsions with aerogel.

emulsion and the results are shown in Fig. 11. The prepared aqueous emulsion of toluene was poured on the aerogel for separation. As shown in Fig. 11(a), the liquid spontaneously penetrated the aerogel and the filtrate was homogeneous, indicating successful emulsion separation. In addition, the optical microscopic images showed the presence of water droplets before filtration which were almost invisible after filtration (Fig. 11(b), (c)).

## CONCLUSIONS

A novel aerogel material with a laminar porous structure was successfully prepared. The optimal aerogels exhibited high porosity (98.3%), strong compressive elasticity, excellent hydrophobic (water contact angle of  $139^\circ$ ) and lipophilic properties. The aerogel also displayed outstanding adsorption capacity and recyclability, which could adsorb oil and organic solvents up to 23–44 times its weight. Meanwhile, after ten adsorption-desorption cycles, the sample could still maintain 71% of its original adsorption capacity. Therefore, the developed aerogel is expected to be an environmentally friendly oil-adsorbing material in environmental protection.

## ACKNOWLEDGEMENTS

Instrument Analysis center of Dalian Polytechnic University is gratefully acknowledged for all the equipment employed. This research was supported by Natural Science Foundation of Liaoning Province (2019-ZD-0923), National Key Research and Development Program of China (No. 2019YFC0605003).

## SUPPORTING INFORMATION

Additional information as noted in the text. This information is available via the Internet at <http://www.springer.com/chemistry/journal/11814>.

## REFERENCES

1. S. Rostami, O. Abessi and H. Amini-Rad, *Mar. Pollut. Bull.*, **138**, 302 (2019).
2. E. M. Soliman, S. A. Ahmed and A. A. Fadl, *J. Environ. Health Sci. Eng.*, **18**, 79 (2020).
3. Y. Wang, K. Lee, D. Liu, J. Guo, Q. Han, X. Liu and J. Zhang, *Environ. Pollut.*, **263**, 114343 (2020).
4. Y. Li, X. Liu, W. Cai, Y. Cao, Y. Sun and F. Tan, *Korean J. Chem. Eng.*, **35**, 1119 (2018).
5. G.-L. Zhuang, S.-Y. Wu, Y.-C. Lo, Y.-C. Chen, K.-L. Tung and H.-H. Tseng, *J. Membr. Sci.*, **605**, 118091 (2020).
6. F. Hashemi, H. Hashemi, M. Shahbazi, M. Dehghani, M. Hoseini and A. Shafeie, *Water Resour. Ind.*, **23**, 100123 (2020).
7. H. Ozgun, M. E. Ersahin, S. Erdem, B. Atay, B. Kose, R. Kaya, M. Altinbas, S. Sayili, P. Hoshan, D. Atay, E. Eren, C. Kinaci and I. Koyuncu, *J. Chem. Technol. Biotechnol.*, **88**, 1576 (2013).
8. M. O. Adebajo, R. L. Frost, J. T. Klopogge, O. Carmody and S. Kokot, *J. Porous Mater.*, **10**, 159 (2003).
9. M. Ma, Y. Chen, X. Zhao, F. Tan, Y. Wang, Y. Cao and W. Cai, *J. Saudi Chem. Soc.*, **24**, 915 (2020).
10. L. Wang, C. Shi, L. Wang, L. Pan, X. Zhang and J.-J. Zou, *Nanoscale*, **12**, 4790 (2020).
11. A. Bayat, S. F. Aghamiri, A. Moheb and G. R. Vakili-Nezhaad, *Chem. Eng. Technol.*, **28**, 1525 (2005).
12. S. J. Teichner, G. A. Nicolaon, M. A. Vicarini and G. E. E. Gardes, *Adv. Colloid Interface Sci.*, **5**, 245 (1976).
13. R. Yogapriya and K. R. D. Kasibhatta, *ACS Appl. Nano Mater.*, **3**, 5816 (2020).
14. J. Kim, H. Kim, G. Baek and C. Lee, *Waste Manage.*, **60**, 322 (2017).
15. A. Arulrajah, T.-A. Kua, C. Suksiripattanapong, S. Horpibulsuk and J. S. Shen, *J. Clean. Prod.*, **162**, 1491 (2017).
16. X. Yue, T. Zhang, D. Yang, F. Qiu and Z. Li, *J. Clean. Prod.*, **199**, 411 (2018).
17. L. Zhang, H. Chen, J. Sun and J. Shen, *Chem. Mater.*, **19**, 948 (2007).
18. Z. Xu, H. Zhou, X. Jiang, J. Li and F. Huang, *Iet Nanobiotechnol.*, **11**, 929 (2017).
19. L. Li, T. Hu, H. Sun, J. Zhang and A. Wang, *ACS Appl. Mater. Interfaces*, **9**, 18001 (2017).
20. C. Wang, G. H. He, J. L. Cao, L. H. Fan, W. Q. Cai and Y. H. Yin, *ACS Appl. Polym. Mater.*, **2**, 1124 (2020).
21. J. Yang, Y. Xia, P. Xu and B. Chen, *Cellulose*, **25**, 3533 (2018).
22. P. S. Brown, O. D. L. A. Atkinson and J. P. S. Badyal, *ACS Appl. Mater. Interfaces*, **6**, 7504 (2014).
23. L. Zhou and Z. Xu, *J. Hazard. Mater.*, **388**, 121804 (2020).
24. A. E. Atabani, S. Shobana, M. N. Mohammed, G. Uguz, G. Kumar, S. Arvindnarayan, M. Aslam and A. a. H. Al-Muhtaseb, *Fuel*, **244**, 419 (2019).
25. N. Belhouchat, H. Zaghouane-Boudiaf and C. Viseras, *Appl. Clay Sci.*, **135**, 9 (2017).
26. Y. Wang, Y. Feng and J. Yao, *J. Colloid Interface Sci.*, **533**, 182 (2019).
27. S.-J. Kim, J.-B. Moon, G.-H. Kim and C.-S. Ha, *Polym. Test.*, **27**, 801 (2008).
28. Q. Cheng, D. Ye, C. Chang and L. Zhang, *J. Membr. Sci.*, **525**, 1 (2017).
29. H. Sehaqui, Q. Zhou and L. A. Berglund, *Compos. Sci. Technol.*, **71**, 1593 (2011).
30. M. Fumagalli, D. Ouhab, S. M. Boisseau and L. Heux, *Biomacromolecules*, **14**, 3246 (2013).
31. L. Zhou, S. Zhai, Y. Chen and Z. Xu, *Polymers*, **11**, 712 (2019).
32. J. T. Korhonen, M. Kettunen, R. H. A. Ras and O. Ikkala, *ACS Appl. Mater. Interfaces*, **3**, 1813 (2011).